Evaluation of ^{11}C-BU99008, a Positron Emission Tomography ligand for the Imidazoline$_2$ binding sites in Rhesus brain

Christine A. Parker[1,2,†], Nabeel Nabulsi[3,†], Daniel Holden[3], Shu-fei Lin[3], Tara Cass[3], David Labaree[3], Steven Kealey[4], Antony D. Gee[5], Stephen M. Husbands[6], Darren Quelch[1], Richard E. Carson[3], David J. Nutt[1], Yiyun Huang[3], Robin J. Tyacke[1]

† These two authors contributed equally to this work.

RUNNING TITLE: Evaluation of ^{11}C-BU99008 in Rhesus

1. Centre for Neuropsychopharmacology, Hammersmith Hospital, Imperial College London, W12 0NN, UK

2. GSK, Global Imaging Unit, Stevenage, SG1 2NY, UK

3. PET Center, Department of Diagnostic Radiology, Yale University, Connecticut, USA

4. Institute of Psychiatry, De Crespigny Park, King's College London, SE5 8AF, UK

5. Division of Imaging Sciences and Biomedical Engineering, King's College London, St Thomas' Hospital, London SE1 7EH, UK

6. Department of Pharmacy and Pharmacology, University of Bath, Bath BA2 7AY, UK

Correspondence to: Dr R Tyacke

Centre for Neuropsychopharmacology, Imperial College London, Burlington Danes Building, Hammersmith Hospital, 160 Du Cane Road, London W12 0NN

e: r.tyacke@imperial.ac.uk

t: +44(0)20 75947047

f: +44(0)20 75946548

WORD COUNT = ~5002

Abstract

The development of a PET radioligand selective for I_2-imidazoline binding sites (I_2BS) would enable, for the first time, specific, measurable *in vivo* imaging of this target protein, along with assessment of alterations in expression patterns of this protein in disease pathophysiology.

Methods: BU99008 was identified as the most promising I_2BS radioligand candidate, and radiolabelled with carbon-11 via methylation. The *in vivo* binding properties of ^{11}C-BU99008 were assessed in rhesus monkeys in order to determine: brain penetration, brain distribution, binding specificity and selectivity (via the use of the unlabelled blockers), and the most appropriate kinetic model for analysing data generated with this PET radioligand.

Results: ^{11}C-BU99008 was demonstrated to readily enter to the brain resulting in a heterogeneous distribution (globus pallidus>cortical regions>cerebellum) consistent with the reported regional I_2BS densities as determined by human tissue section autoradiography and preclinical *in vivo* PET studies in the pig. *In vivo* competition studies revealed ^{11}C-BU99008 displayed reversible kinetics specific for the I_2BS. The MA1 multi-linear model was the most appropriate analysis method for this PET radioligand in this species. The selective, I_2BS blocker, BU224, was shown to cause a saturable, dose-dependent decrease in ^{11}C-BU99008 binding in all regions of the brain assessed, further demonstrating the heterogeneous distribution of I_2BS protein in the rhesus brain and binding specificity for this radioligand.

Conclusion: These data demonstrate ^{11}C-BU99008 represents a specific and selective PET radioligand for imaging and quantifying the I_2BS, *in vivo*, in rhesus monkey. Further work is underway to translate the use of ^{11}C-BU99008 to the clinic.

Keywords: Imidazoline$_2$ binding site, I_2BS, positron emission tomography, PET, BU99008

Introduction

The ability of the α_2-adrenoceptor agonist clonidine and the antagonist idazoxan, to label a sub-population of binding sites, not displaceable by the endogenous ligand noradrenaline, led to the discovery of the imidazoline binding sites some 20 years ago. These binding sites have subsequently been divided into three groups: the imidazoline$_1$ binding site that is preferentially labelled by ^{3}H-clonidine, the imidazoline$_2$ binding site (I_2BS) that is preferentially labelled by ^{3}H-idazoxan, and the imidazoline$_3$ binding site which is an atypical imidazoline site found on pancreatic β-cells (for review see (*1*)).

I_2BS are known to reside on the mitochondrial membranes of astrocytes (*2*). Changes in post-mortem binding density of the I_2BS has implicated them in a range of psychiatric conditions such as depression and addiction, along with neurodegenerative disorders such as Alzheimer's disease and Huntington's chorea (*3*). Functional interactions in preclinical models have also been shown in relation to the opioid system, where I_2BS ligands have been shown to affect tolerance to morphine (*4*) and alleviate some of the morphine withdrawal syndrome in rats (*5*). I_2BS ligands have also been shown acutely to affect feeding and appetite by an as yet undetermined mechanism (*6*). The location of I_2BS on glial cells and the possibility that they may in some way regulate glial fibrillary acidic protein (*7*) have led to increased interest into the role of I_2BS and I_2BS ligands in conditions characterised by marked gliosis. The density of I_2BS has been shown to increase in Alzheimer's disease post mortem (*3*), and it has also been suggested that I_2BS may be a marker for human glioblastomas (*8*). Subsequent publications added weight to this argument showing that the density of I_2BS is increased *in vivo* with heat-induced gliosis (*9*). Additionally, Callado and coworkers have shown not only an increase in the I_2BS in human gliomas but this increase in binding sites was correlated with the severity and malignancy of the glioma (*10*).

Positron emission tomography (PET) is an *in vivo* imaging technique that uses radioligands as selective molecular probes to map the location and density of specific proteins. The development of a selective I_2BS PET radioligand would

allow for the characterisation of I_2BS *in vivo* and their regulation in disease states. A number of ligands selective for I_2BS have been reported, but only two potential PET radioligands have been reported to date: the radiosynthesis of ^{11}C-benazoline, but its study *in vivo* has not been reported (*11*) and radiosynthesis and *in vivo* imaging evaluation of ^{11}C-FTIMD in non-human primate (*12*) although the specific binding signal appears to be low for this radioligand.

We have recently reported the synthesis, *in vitro* and *in vivo* evaluation and radiosynthesis of a PET radioligand for the I_2BS, ^{11}C-BU99008 (*13, 14*). In this manuscript, we report the preclinical *in vivo* evaluation of ^{11}C-BU99008, for imaging I_2BS, in rhesus monkey brain.

Materials and Methods

Chemicals

^{3}H-BU99008 (SA=1.04TBq/mmol) was custom synthesised by Sibtech. Challenge drugs moclobemide and lazabemide were obtained from commercial suppliers: Sigma-Aldrich Company Ltd. and Tocris Biosciences. Dr Husbands synthesized the BU224. All other chemicals and reagents were purchased from commercial suppliers and used without further purification.

Animals

All experiments in animals were carried out in accordance with the UK Animals (Scientific Procedures) Act 1986. PET imaging experiments in rhesus monkeys were conducted in accordance with a protocol approved by the Yale University Institutional Animal Care and Use Committee.

In Vitro Competition Binding Studies

Membrane preparation, competition binding studies and data analysis were conducted as previously described (*13*) with the following alterations. Rat (male, Wistar, 250-300g) and Cynomologus monkey brains were used and resulting membrane preparations stored at -80^{o}C. The displacement binding studies for the ^{3}H-BU99008 (1nM) were conducted at 37°C in assay buffer (50mM TRIS-HCl, 140mM NaCl, 1.5mM $MgCl_2$, 5mM KCl, 1.5mM $CaCl_2$, pH7.4), and radioactivity was determined using a Tricarb 2900 β-counter. Protein content was determined using a Pierce bicinchoninic acid kit.

PET Imaging Studies in Rhesus Monkeys

Radiochemistry. ^{11}C-BU99008 was prepared by *N*-alkylation of the desmethyl precursor BU99007 with ^{11}C-CH_3I in the AutoLoop synthesis module (Bioscan). A description of the synthetic methods can be found in supplementary information (Supplementary Figure 1 (supplemental materials are available online only at http://jnm.snmjournals.org)).

Study Design. Two Rhesus monkeys (*Macaca mulatta*; female, ~6kg, 7 years and female, ~7kg, 8 years) were used, with scanning days at least 14 days apart. Each animal had five scanning days. Each scanning day consisted of a baseline scan with ^{11}C-BU99008 (120min); following this, animals received an i.v. injection of blocking drug over a 10min period, ~10min prior to initiation of a second scan with ^{11}C-BU99008 (120min), to determine binding specificity and selectivity of the radioligand (Supplementary Table 1). Administration of the specific I_2BS ligand, BU224, was: monkey one, 0.01, 0.03 and 0.3mg/kg, and monkey two, 0.01, 0.03, 0.1mg/kg. To assess the selectivity of binding to I_2BS, both animals received an injection of the reversible MAO_A inhibitor, moclobemide (1mg/kg) and the reversible MAO_B inhibitor, lazabemide (0.5mg/kg). Data acquisition started simultaneously with ligand injection. Vital signs were monitored at least four times per hour, and more frequently following injection of tracer and blocking drugs.

MRI Imaging. Images were acquired for each monkey on a Siemens 3.0-T Trio scanner, using an extremity coil. T_1-weighted images were acquired in the coronal plane with a spin-echo sequence (TE=3.34, TR=2530, flip angle=7°, section thickness=0.50mm, field of view=140mm, image matrix=256×256×176 pixels, matrix size=0.547×0.547×0.500mm). Whole brain image was cropped to 176×176×176 pixels using MEDx software (Medical Numerics) before co-registration with PET image data.

PET Imaging Procedures. Animals were sedated with an intramuscular injection of ketamine hydrochloride (10±2mg/kg), ~2h prior to the start of scanning, transported to the PET facility, anaesthetized using isofluorane, intubated and maintained on oxygen and 1.5–2.5% isofluorane throughout the study. PET scans were performed on the FOCUS 220 PET scanner (Siemens Preclinical Solutions), with a reconstructed image resolution of ~1.5mm. Following a transmission scan, 170±14MBq (4.6±0.4mCi; mass dose=0.08±0.02μg/kg) of ^{11}C-BU99008 was injected over 3min. List-mode data were acquired for 120min and binned into sinograms with the following frame timing: 6×30s; 3×1min; 2×2min; 22×5min.

Dynamic scan data were reconstructed with a filtered-back projection algorithm with corrections for attenuation, normalization, scatter, and randoms.

Arterial Blood Sampling. Arterial blood samples were collected for the determination of: whole blood and plasma input functions, and metabolite analysis and plasma free fraction (f_p) of ^{11}C-BU99008. These procedures are described in detail in the supplementary information.

Regional Time-Activity Curve Computation. An existing region of interest (ROI) map defined on a template brain (a representative MR image of a rhesus brain) was used. The following, a priori defined, ROI were examined: cingulate, frontal, insula, and occipital cortex, brainstem, pons, cerebellum, caudate, putamen, globus pallidus and thalamus. A nonlinear transformation was estimated using the Bioimagesuite software (http://www.bioimagesuite.org/) to transfer the ROI template to the MR image of each animal used during this study. These regions were then transferred to the PET images based on a rigid transformation matrix (*15*), and used to generate time-radioactivity curves (TAC).

Kinetic Modeling. Regional TACs were analysed using one- and two-tissue compartment models (1TC and 2TC) and multi-linear analysis (MA1) (*16*) to calculate regional distribution volume (V_T). MA1 is a linear method related to Logan analysis, but with less noise-induced bias. Like Logan analysis, data are fitted starting at a specified time, t*; here t^*=20min. The optimal model was based on quality of fit, and the uncertainty (standard error) of the V_T parameter estimate. For blocking studies, since there was no suitable reference region, a graphical method was used to calculate the non-displaceable volume of distribution (V_{ND}) and global and regional receptor occupancy (*17*). Receptor occupancy data from different blocking drug doses was fitted to a one-site binding E_{max} model where occupancy values (*Occ*) are plotted versus administered dose (*d*); where $Occ = d/(d + ED_{50})$, in order to derive the blocking dose needed to induce 50% global receptor occupancy (ED_{50}). Regional values were also derived from receptor occupancy calculated from the V_T values at baseline and at various blocking doses

using the equation above modified to add a parameter to permit maximum reduction in V_T of <100%, i.e., accounting for V_{ND}.

RESULTS

In vitro Competition Binding Studies

^{3}H-BU99008 *in vitro* competition data demonstrated a two-site fit to the rodent brain with BU224 exhibiting an $IC_{50(High)}$ value of 50.5±12.9nM (Table 1), consistent with previous data (*13*). In contrast, competition of BU224 in cynomologus brain yielded a single site fit with an IC_{50} value of 130.2±33.9nM (Table 1). Competition of ^{3}H-BU99008 from both rat and cynomologus brains by the MAO_B inhibitor, lazabemide, exhibited very poor inhibition of binding and the MAO_A inhibitor, moclobemide, showed no inhibition at the highest concentration used (Table 1).

Radiochemistry

Injection ready ^{11}C-BU99008 was successfully synthesised with a chemical yield of 32±17% (decay-corrected), radiochemical purity of >99%, and a specific activity of 146±33MBq/nmol (3.95±0.90mCi/nmol, n=19) at the end of synthesis. The identity of the radiolabelled product was confirmed by co-injection with a sample of authentic BU99008, which, under the same elution conditions, showed an identical retention time.

In vivo Blood Data

Free fraction (f_P) of ^{11}C-BU99008 in the plasma was high, at 0.68±0.07 (n=19). The amount of total radioactivity measured in plasma was similar between baseline scans and following administration of either the MAO inhibitors or the I_2BS inhibitor (Figure 1A). In addition, radio-HPLC analysis revealed ^{11}C-BU99008, under baseline conditions, to be rapidly metabolised in plasma, with the parent compound representing about 50% of the total radioactivity 20min following administration (Figure 1B). However, there was a small decrease in parent fraction of ^{11}C-BU99008 following administration of all three inhibitors compared with data acquired under baseline conditions, where the parent compound represented about 50% of the total radioactivity at 15min following administration (Figure 1B).

***In vivo* PET Studies**

Representative baseline PET images and corresponding TACs for ^{11}C-BU99008 uptake into the rhesus brain are given in Figures 2B and 3A, respectively. ^{11}C-BU99008 readily entered the brain with the highest uptake observed in the globus pallidus, caudate and thalamus, with moderate uptake in the cortical and putamen regions, and lowest uptake in the cerebellum and occipital cortex. Peak radioactivity concentrations were observed approximately 15–25min after administration of ^{11}C-BU99008, followed by a slow washout from all regions (Figure 3A).

The regional TACs were analysed by the reversible 1TC and 2TC models as well as by the MA1 model, (*16*). The 2TC model produced good fits to the data, but over 20% of fits to baseline data had unreliable V_T estimates, i.e., standard errors (%SE) >20%. Poor reliability occurred most often in smaller, noisier regions and in baseline scans or scans with little effective blockade (see below). The 1TC model showed clear lack of fit in most cases. Also, the V_T values from 1T underestimated those from 2TC by 10-40% (excluding 2TC values with high %SE), with the relationship of $V_{T(1T)}=0.87 \times V_{T(2T)} - 4.2$, $r^2=0.92$. The MA1 method produced good fits and stable estimates for V_T with small differences in V_T values using different t* values from 20 and 40min. In the cases where 2TC values had %SE <20%, the relationship between MA1 and 2TC values was $V_{T(MA1)}=0.94 \times V_{T(2T)} - 1.3$, $r^2=0.97$). Based on the bias from 1TC fits, and the numerous cases of high %SE from 2TC, MA1 with t*=20min, was chosen as the model of choice for derivation analysis.

Table 2 lists MA1-derived regional V_T values from individual baseline scans. The baseline data acquired from the two rhesus monkeys were demonstrated to be reproducible and consistent throughout the course of the study (Figure 4). Using the MA1 model with t*=20min, baseline V_T values were highest in the globus pallidus (114.2±24.0mL/cm), caudate (109.7±13.7mL/cm) and thalamus (96.3±8.1mL/cm) and lowest in the cerebellum (48.1±4.8mL/cm). This rank order of regional V_T for ^{11}C-BU99008 from the baseline data (globus pallidus>cortex>cerebellum, Table 2) is consistent with reported I_2BS densities and

distribution determined by tissue-section autoradiography in humans (*18*) and *in vivo* pig PET (*14*). Furthermore, the mean rhesus V_T values were significantly correlated (r^2=0.72; P<0.05) with the mean V_T values from our previous *in vivo* porcine ^{11}C-BU99008 PET data ((*14*) and unpublished data from the porcine study) (inset, Figure 4).

In vivo blocking studies utilising the MAO_A and MAO_B inhibitors, moclobemide and lazabemide, respectively, did not cause any significant change in binding signal of ^{11}C-BU99008 to any regions studied (Figures 2C, 2E, and Supplementary Figure 2). *In vivo* competition using ^{11}C-BU99008 plus increasing doses of the selective I_2BS blocker, BU224, yielded a dose-dependent decrease in uptake of ^{11}C-BU99008 in all regions studied. The highest dose administered (0.3mg/kg) yielded an apparent near-to-full blockade, suggesting high selectivity of this radioligand for the I_2BS (Figures 2G, 3B, and 5, Table 3). The presence of a dose-dependent decrease in binding in the cerebellum suggests this is not a suitable reference region for analysis of ^{11}C-BU99008.

A global receptor occupancy measure was calculated for the BU224 studies using the occupancy plot (*17*). Occupancy values ranged from 25-35% for the lowest dose of BU224 (0.01mg/kg) to 93% for the highest dose (0.3mg/kg). These occupancies were plotted vs. administered dose (*d*) in Figure 6 with a fit to the equation Occ = $d/(d + ED_{50})$, which yielded an ED_{50} estimate of 0.022mg/kg for the whole brain (Table 3).

Regional ED_{50} values for BU224 were also calculated for the globus pallidus, frontal cortex and cerebellum using the percentage reduction in V_T instead of the estimated global occupancy value (Supplementary Figure 3A, B, C). Calculated regional ED_{50} values were 0.017mg/kg for globus pallidus, 0.017mg/kg for frontal cortex, and 0.016mg/kg for the cerebellum (Supplementary Figure 3, Table 3).

DISCUSSION

This paper describes the radiosynthesis of ^{11}C-BU99008 and its characterisation as a novel PET radioligand for the quantification of central I_2BS *in vivo* in rhesus monkeys.

BU99008 was selected as the most suitable compound for radiolabelling with a PET radioisotope for imaging the I_2BS, as reported previously by our group (*13*). In addition, BU99008 exhibited selectivity and nanomolar affinity for the I_2BS in the rodent and cynomologus brain (Table 1). Interestingly, a two-site model fit was preferred for the rodent and a one-site fit for the cynomologus brain tissue, suggesting that, in the rodent brain, BU99008 exhibits a degree of affinity for a second binding site which may be unrelated to the I_2BS, possibly reflecting a monoamine oxidase binding component (*19*). Importantly, due to the nature of the I_2BS being co-localised with monoamine oxidases (MAO) on the outer membrane mitochondrial enzymes (*20*), it was essential to investigate the relative affinities of selective MAO_A and MAO_B inhibitors for the I_2BS in order to proceed. *In vitro* studies using cynomologus brain demonstrated MAO inhibitors to possess a low affinity for the I_2BS in (Table 1). However in the rodent brain tissue, the MAO_B inhibitor possessed a similar affinity for the low affinity binding site exhibited previously in the rodent brain by BU224 (Table 1). These data confirm the notion that the high affinity binding component, *in vitro*, in both the rat and cynomologus brain is expected to represent the I_2BS.

In view of these *in vitro* data, and combined with a successful radiolabelling feasibility assessment, we progressed the development of BU99008 as a PET ligand via evaluation in porcine brain, *in vivo* (*14*). In that study, ^{11}C-BU99008 demonstrated reversible kinetics and a brain distribution consistent with the known binding site densities and localisation for the I_2BS protein, and a dose-dependent decrease in V_T following administration of the selective I_2BS blocker, BU224. Further studies in pig showed a small, but relevant, binding component associated with MAO (manuscript in preparation). Therefore, given that relative expression levels of I_2BS and MAO differs from species to species, in order to progress

^{11}C-BU99008 for use in human studies we decided to assess this PET ligand further, preclinically, in rhesus monkey, since we predict human brain uptake and *in vivo* binding characteristics of this particular PET ligand would be more similar to rhesus than porcine. BU99008 was successfully radiolabelled with carbon-11 with good reproducibility, radiochemical yields and high specific activities.

After injection into a rhesus monkey, the radioligand ^{11}C-BU99008 metabolised fairly quickly, with only ~30% of parent compound remaining at 30min post injection. A slight acceleration in metabolism was also observed when blocking agents were given before ^{11}C-BU99008 injection but this effect was modest and unlikely to affect the usability of this ligand.

In monkey brain ^{11}C-BU99008 displayed differential regional uptake. This heterogeneous distribution of ^{11}C-BU99008 exhibited the following rank order: globus pallidus and other basal ganglia regions>cortex>cerebellum, consistent with the known I_2BS densities and results from human tissue-section autoradiography (*18*) and porcine PET imaging experiments (*14*). While the cerebellum showed the lowest brain uptake there was still a decrease in V_T values after BU224 blockade (Figure 4), indicating cerebellum would be unsuitable as a reference region. This was consistent with the findings of our previous study in pig (*14*).

An assessment of the intra-subject variability was performed that yielded low to moderate variability in the V_T values obtained for each ROI studied for each subject across multiple baseline scans (Figure 4). Furthermore, comparison of inter-species variability between the rhesus monkeys used in this study and pigs used previously by our group with this PET radioligand (*14*), demonstrated a significant correlation (inset, Figure 4), suggesting a degree of correspondence between these two species for the I_2BS, albeit ^{11}C-BU99008 appears to be affected by MAO inhibitors in the porcine which is a phenomenon not exhibited in the rhesus (manuscript in preparation).

The effects of the MAO_A inhibitor, moclobemide, and the MAO_B inhibitor, lazabemide, on ^{11}C-BU99008 binding were determined *in vivo*, in rhesus monkey and found to cause no significant decrease in V_T in any of the ROIs assessed (Supplementary Figure 2). This key finding suggests that in rhesus monkey brain any contribution of the ^{11}C-BU99008 signal due to binding to MAO is small or negligible and would not be expected to cause any significant interference with the assessment of I_2BS binding signal in this species.

Following administration of increasing blocking doses of BU224, a dose-dependent decrease in ^{11}C-BU99008 V_T was observed in all regions of the rhesus brain (Figure 5), confirming the absence of a reference region for this PET radioligand, and remaining consistent with the known distribution profile for I_2BS in the brain. The dose-dependent decrease in V_T observed for all ROI studied is not thought to represent a global change unrelated to the specific binding of ^{11}C-BU99008 and the blocking by BU224 given that: (a) a heterogeneous signal was observed across the ROI under baseline conditions, (b) differential levels of decrease in V_T values were observed for each region following increasing doses of BU224, and (c) a plateau at a V_T value of ~20mL/cm was achieved for all ROI following the highest dose of BU224 administered (0.3mg/kg; Figure 5). Additionally, the dose-dependent blockade by the selective I_2BS inhibitor in the rhesus brain confirmed the specificity of ^{11}C-BU99008 for the I_2BS and demonstrated a blockade of ~90% across all ROI at the highest dose administered (0.3mg/kg). Interestingly, the *in vivo* ED_{50} of BU224 generated across all brain regions was consistent with the presence of one binding site and generated a value of 0.022mg/kg (Figure 6), which is consistent with the known *in vitro* and *ex vivo* properties of this compound (*5*).

Given these data, we predict that ^{11}C-BU99008 should demonstrate a similar binding distribution profile in the human brain to that observed from this study in rhesus monkey, where the rank order of regional brain uptake for this ligand would be expected to be globus pallidus>cortical regions>cerebellum. For modelling purposes, since the multi-linear analysis method, MA1, consistently produced good

fits to the data along with reliable and stable estimates of V_T for all regions of the rhesus brain studied, the use of this particular model for analysis of PET data generated using ^{11}C-BU99008 should be considered in future studies. Work is underway to assess the utility of ^{11}C-BU99008 as a PET ligand for *in vivo* imaging and quantification of I_2BS in the human population, and if deemed useful, its applicability for determining alterations in I_2BS density and distribution in known disease states will be investigated.

Conclusions

This manuscript reports the radiolabelling and pharmacological investigation of ^{11}C-BU99008 as a novel I_2BS PET radioligand in rhesus monkeys. *In vivo* distribution of ^{11}C-BU99008 in the rhesus monkey brain demonstrated the following rank order of regional uptake: globus pallidus>cortex>cerebellum, consistent with the known distribution profile of the I_2BS. ^{11}C-BU99008 displayed reversible kinetics and specificity for the I_2BS, with the MA1 model representing the most appropriate analysis method for the derivation of binding parameters for this PET radioligand. The data reported here provides evidence for ^{11}C-BU99008 to represent a potentially useful PET imaging tool for probing the I_2BS. Work is underway in order to progress ^{11}C-BU99008 for assessment of its clinical utility as a PET radioligand for I_2BS.

Acknowledgments

We thank the MRC (G0801501) and GSK for funding the study; Roger Gunn and Eugenii Rabiner for interesting discussions and their continued support of this study.

References

1. Eglen RM, Hudson AL, Kendall DA, et al. 'Seeing through a glass darkly': casting light on imidazoline 'I' sites. *Trends Pharmacol Sci.* 1998;19:381-390.

2. Regunathan S, Feinstein DL, Reis DJ. Expression of non-adrenergic imidazoline sites in rat cerebral cortical astrocytes. *J Neurosci Res.* 1993;34:681-688.

3. Garcia-Sevilla JA, Escriba PV, Guimon J. Imidazoline receptors and human brain disorders. *Ann N Y Acad Sci.* 1999;881:392-409.

4. Ruiz-Durantez E, Torrecilla M, Pineda J, Ugedo L. Attenuation of acute and chronic effects of morphine by the imidazoline receptor ligand 2-(2-benzofuranyl)-2-imidazoline in rat locus coeruleus neurons. *Br J Pharmacol.* 2003;138:494-500.

5. Hudson AL, Gough R, Tyacke R, et al. Novel selective compounds for the investigation of imidazoline receptors. *Ann N Y Acad Sci.* 1999;881:81-91.

6. Hudson AL, Nutt DJ, Husbands SM. Imidazoline receptors and their role in depression. *Pharma News.* 2001;8:26-32.

7. Olmos G, Alemany R, Escriba PV, Garcia-Sevilla JA. The effects of chronic imidazoline drug treatment on glial fibrillary acidic protein concentrations in rat brain. *Br J Pharmacol.* 1994;111:997-1002.

8. Martin-Gomez JI, Ruiz J, Callado LF, et al. Increased density of I2-imidazoline receptors in human glioblastomas. *Neuroreport.* 1996;7:1393-1396.

9. Martin-Gomez JI, Ruiz J, Barrondo S, Callado LF, Meana JJ. Opposite changes in imidazoline I2 receptors and alpha2-adrenoceptors density in rat frontal cortex after induced gliosis. *Life Sci.* 2005;78:205-209.

10. Callado LF, Martin-Gomez JI, Ruiz J, Garibi JM, Meana JJ. Imidazoline I(2) receptor density increases with the malignancy of human gliomas. *J Neurol Neurosurg Psychiatry.* 2004;75:785-787.

11. Roeda D, Hinnen F, Dolle F. Radiosynthesis of a 2-substituted 4,5-dihydro-1H-[2-C-11] imidazole: the I-2 imidazoline receptor ligand [Cl-11 benazoline. *J Labelled Compd Rad.* 2003;46:1141-1149.

12. Kawamura K, Maeda J, Hatori A, et al. In vivo and in vitro imaging of I(2) imidazoline receptors in the monkey brain. *Synapse.* 2011;65:452-455.

13. Tyacke RJ, Fisher A, Robinson ES, et al. Evaluation and initial in vitro and ex vivo characterization of the potential positron emission tomography ligand, BU99008 (2-(4,5-dihydro-1H-imidazol-2-yl)-1- methyl-1H-indole), for the imidazoline(2) binding site. *Synapse.* 2012;66:542-551.

14. Kealey S, Turner EM, Husbands SM, et al. Imaging imidazoline-I2 binding sites in porcine brain using 11C-BU99008. *J Nucl Med.* 2013;54:139-144.

15. Sandiego CM, Weinzimmer D, Carson RE. Optimization of PET-MR registrations for nonhuman primates using mutual information measures: a Multi-Transform Method (MTM). *Neuroimage.* 2013;64:571-581.

16. Ichise M, Toyama H, Innis RB, Carson RE. Strategies to improve neuroreceptor parameter estimation by linear regression analysis. *J Cereb Blood Flow Metab.* 2002;22:1271-1281.

17. Cunningham VJ, Rabiner EA, Slifstein M, Laruelle M, Gunn RN. Measuring drug occupancy in the absence of a reference region: the Lassen plot re-visited. *J Cereb Blood Flow Metab.* 2010;30:46-50.

18. De Vos H, Convents A, De Keyser J, et al. Autoradiographic distribution of alpha 2 adrenoceptors, NAIBS, and 5-HT1A receptors in human brain using [3H]idazoxan and [3H]rauwolscine. *Brain Res.* 1991;566:13-20.

19. Paterson LM, Tyacke RJ, Robinson ES, Nutt DJ, Hudson AL. In vitro and in vivo effect of BU99006 (5-isothiocyanato-2-benzofuranyl-2-imidazoline) on I2 binding in relation to MAO: evidence for two distinct I2 binding sites. *Neuropharmacology.* 2007;52:395-404.

20. Bonivento D, Milczek EM, McDonald GR, et al. Potentiation of ligand binding through cooperative effects in monoamine oxidase B. *J Biol Chem.* 2010;285:36849-36856.

Tables

Table 1. In vitro I_2BS binding affinities of the blocking drugs in rat and non-human primate brain using ^{3}H-BU99008.

Protein Target	Blocking drug	IC_{50}±SD (nM)	
		Rat	Cynomologus
I_2BS	BU224	50.5±12.9 (high) 9596±2494 (low)	130.2±33.9
MAO_A	Moclobemide	>100,000	>100,000
MAO_B	Lazabemide	6445±1733	17370±2068

Displacement of ^{3}H-BU99008 by BU224 was best fit to a 2-site model in rat only, for all other instances the data was best fit to a 1-site model; (n=4).

Table 2. Baseline regional V_T values (mL/cm) for ^{11}C-BU99008 using MA1. Values are computed with t*=20min (n=8).

Brain Region	MA1 V_T (Mean±SD)
Globus Pallidus	114.2±24.0
Caudate	109.7±13.7
Thalamus	96.3±8.1
Putamen	75.7±7.8
Frontal Cortex	75.1±14.2
Cingulate Cortex	85.5±13.0
Occipital Cortex	50.5±7.3
Insula Cortex	76.3±9.2
Pons	70.1±6.9
Brainstem	75.2±8.5
Cerebellum	48.1±4.8

Table 3. Calculated fraction of I_2-BS occupied by BU224 using ^{11}C-BU99008

BU224 Dose	Percentage Occupancy							
(mg/kg)	Whole Brain		Globus Pallidus		Frontal Cortex		Cerebellum	
0.01	35(1)	25(2)	38(1)	32(2)	32(1)	24(2)	30(1)	27(2)
0.03	54(1)*	66(2)	50(1)*	61(2)	48(1)*	65(2)	47(1)*	54(2)
0.1	81(2)		74(2)		73(2)		64(2)	
0.3	93(1)		85(1)		75(1)		72(1)	
ED_{50}	0.022		0.017		0.017		0.016	

Number in parentheses indicates the animal used to derive the value: monkey 1, monkey 2. Whole brain occupancy was calculated using the occupancy plot (*17*) and is derived from the slope for all reported brain regions. Values calculated from the V_T determined using the MA1 model. *Percentage occupancies generated from an averaged composite of baseline scans for monkey 1 due to failure to obtain a baseline scan on this study day.

Figure legends

Figure 1. Mean total plasma radioactivity (panel A) and metabolite data (panel B) for ^{11}C-BU99008 scan. Symbols represent: baseline scan data ● ; blocking scan data using MAO inhibitors △ ; blocking scan data using BU224 □ . Each point represents the mean of all the scans in that group, vertical bars represent the standard deviation.

Figure 2. Representative coronal, transverse, and sagittal images of ^{11}C-BU99008 uptake in rhesus brain. Images are summed from 30-45min following radioligand injection and are displayed as SUVs. A: structural MRI. B,C: baseline and moclobemide pre-block (1mg/kg). D,E: baseline and lazabemide pre-block (0.5mg/kg). F,G: baseline and BU224 pre-block (0.3mg/kg). Paired scans, (B,C), (D,E), and (F,G), were performed on the same day.

Figure 3. Representative time–activity curves for ^{11}C-BU99008 in selected ROIs in rhesus brain. A: Baseline ^{11}C-BU99008 scan. B: ^{11}C-BU99008 scan after administration of BU224 (0.3mg/kg). The symbols represent: Caudate ■ ; Cerebellum □ ; Frontal cortex △ ; Globus pallidus ▼ ; Occipital cortex ◇ ; Putamen ○ ; Thalamus + .

Figure 4. Bar chart showing the regional distribution volume (V_T) of ^{11}C-BU99008 from two animals (monkey 2, open and monkey 1, filled bars). These represent the mean±SD from four separate baseline scans. The insert shows the significant correlation (r^2=0.72; P<0.05) between the mean V_T from this study (both animals) and the pig (n=3; (*14*) and unpublished data from the pig study). Regional V_T values were generated using the MA1 model (t*=20min) for the rhesus data and the 1TC model for the porcine data.

Figure 5. Bar chart showing the regional distribution volume (V_T) of ^{11}C-BU99008 and the effect of increasing doses of the I_2BS ligand BU224: 0.01mg/kg (striped);

0.03mg/kg (chequered); 0.1mg/kg (clear); 0.3mg/kg (grey) and baseline (black). The bars represent the mean±SD; V_T generated using the MA1 model.

Figure 6. Dose dependent occupancy by BU224 in whole brain, occupancy calculated using the occupancy plot (*17*) ED_{50}=0.022mg/kg). V_T data generated using the MA1 model; monkey 1 ● , monkey 2 ○ .

Figure 1. Mean total plasma radioactivity (panel A) and metabolite data (panel B) for ^{11}C-BU99008 scan. Symbols represent: baseline scan data ● ; blocking scan data using MAO inhibitors △ ; blocking scan data using BU224 □ . Each point represents the mean of all the scans in that group, vertical bars represent the standard deviation.

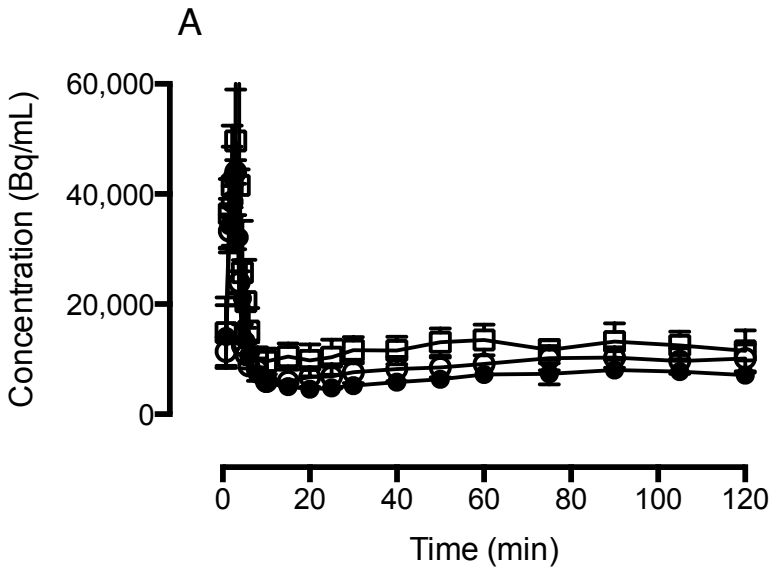

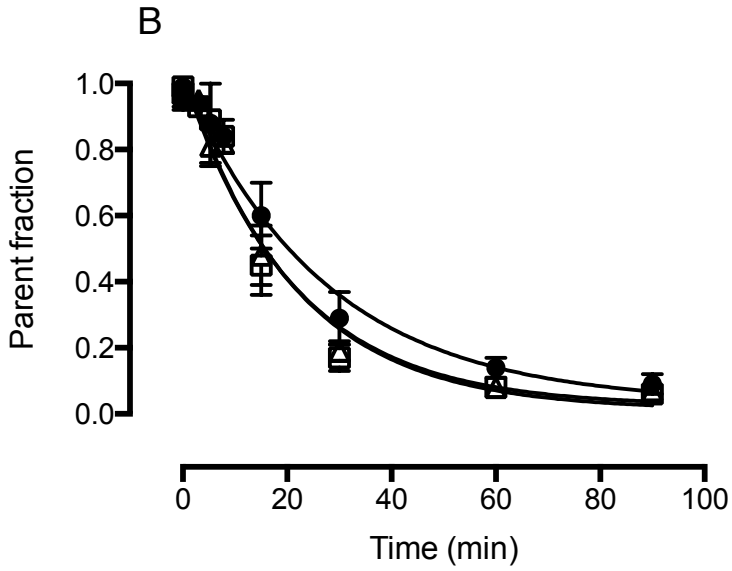

Figure 2. Representative coronal, transverse, and sagittal images of ^{11}C-BU99008 uptake in rhesus brain. Images are summed from 30-45min following radioligand injection and are displayed as SUVs. A: structural MRI. B,C: baseline and moclobemide pre-block (1mg/kg). D,E: baseline and lazabemide pre-block (0.5mg/kg). F,G: baseline and BU224 pre-block (0.3mg/kg). Paired scans, (B,C), (D,E), and (F,G), were performed on the same day.

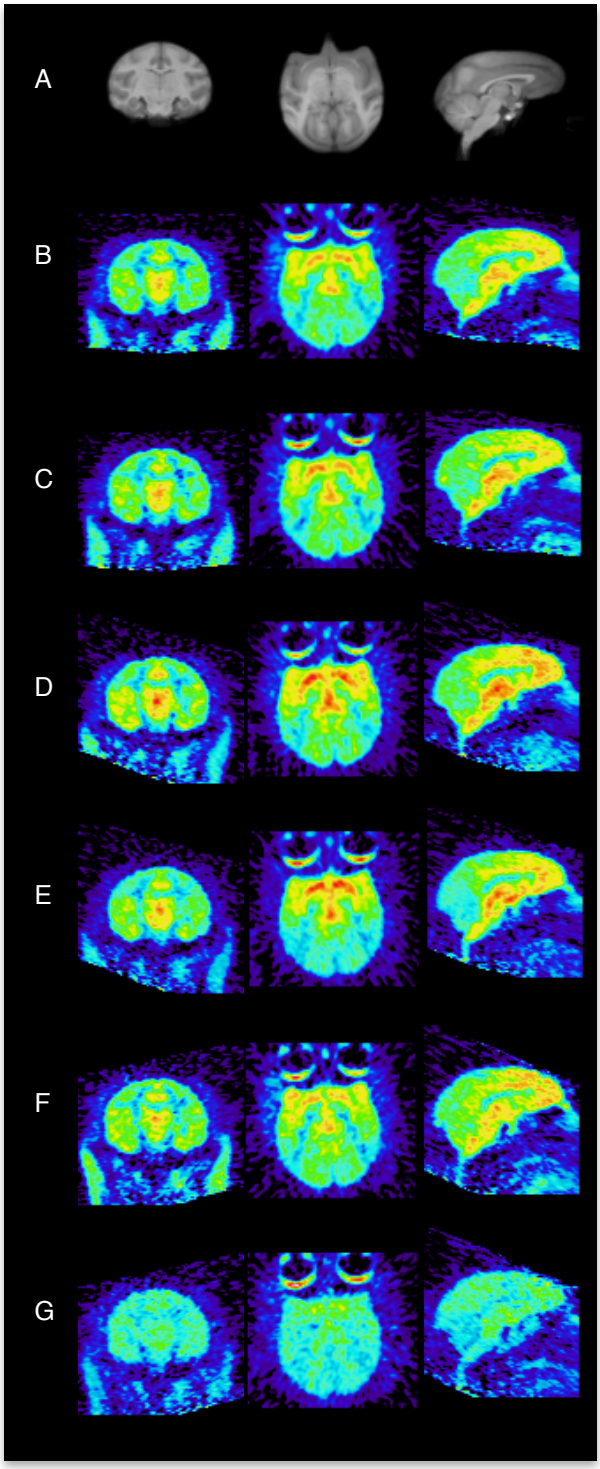

Figure 3. Representative time–activity curves for ^{11}C-BU99008 in selected ROIs in rhesus brain. A: Baseline ^{11}C-BU99008 scan. B: ^{11}C-BU99008 scan after administration of BU224 (0.3mg/kg). The symbols represent: Caudate ■ ; Cerebellum □ ; Frontal cortex △ ; Globus pallidus ▼ ; Occipital cortex ◇ ; Putamen ○ ; Thalamus + .

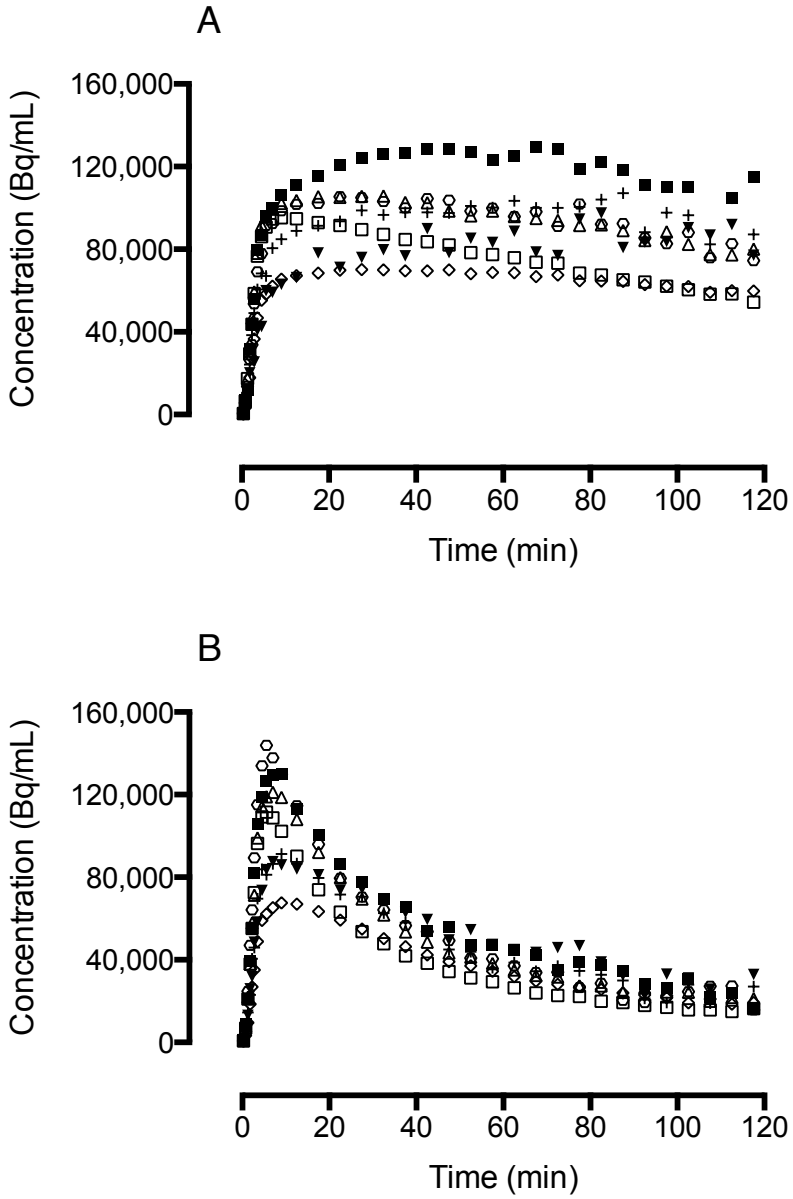

Figure 4. Bar chart showing the regional distribution volume (V_T) of ^{11}C-BU99008 from two animals (monkey 2, open and monkey 1, filled bars). These represent the mean±SD from four separate baseline scans. The insert shows the significant correlation (r^2=0.72; P<0.05) between the mean V_T from this study (both animals) and the pig (n=3; {Kealey, 2013 #910} and unpublished data from the pig study). Regional V_T values were generated using the MA1 model (t*=20min) for the rhesus data and the 1TC model for the porcine data.

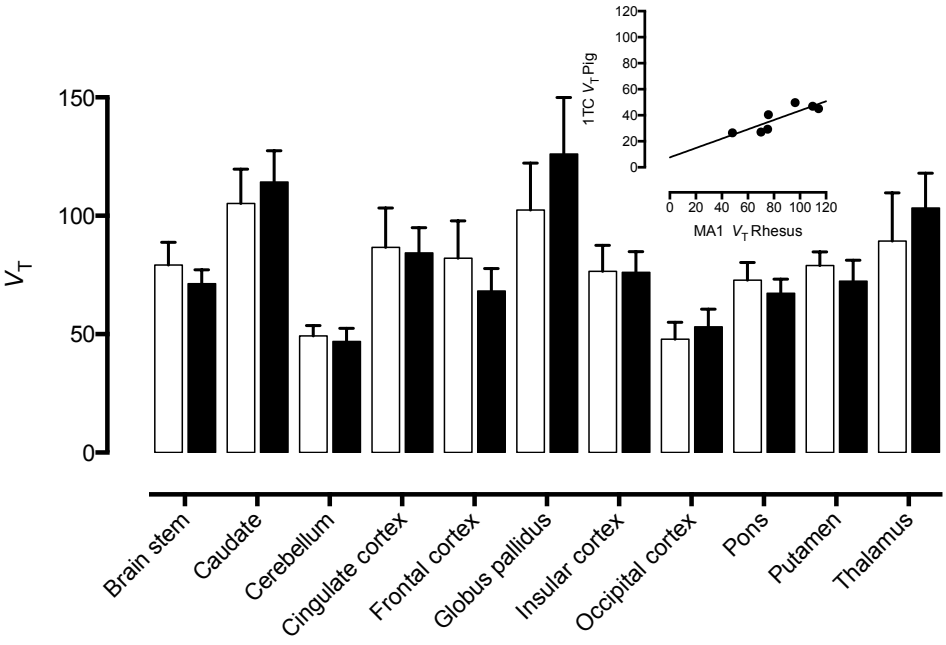

Figure 5. Bar chart showing the regional distribution volume (V_T) of ^{11}C-BU99008 and the effect of increasing doses of the I_2BS ligand BU224: 0.01mg/kg (striped); 0.03mg/kg (chequered); 0.1mg/kg (clear); 0.3mg/kg (grey) and baseline (black). The bars represent the mean±SD; V_T generated using the MA1 model.

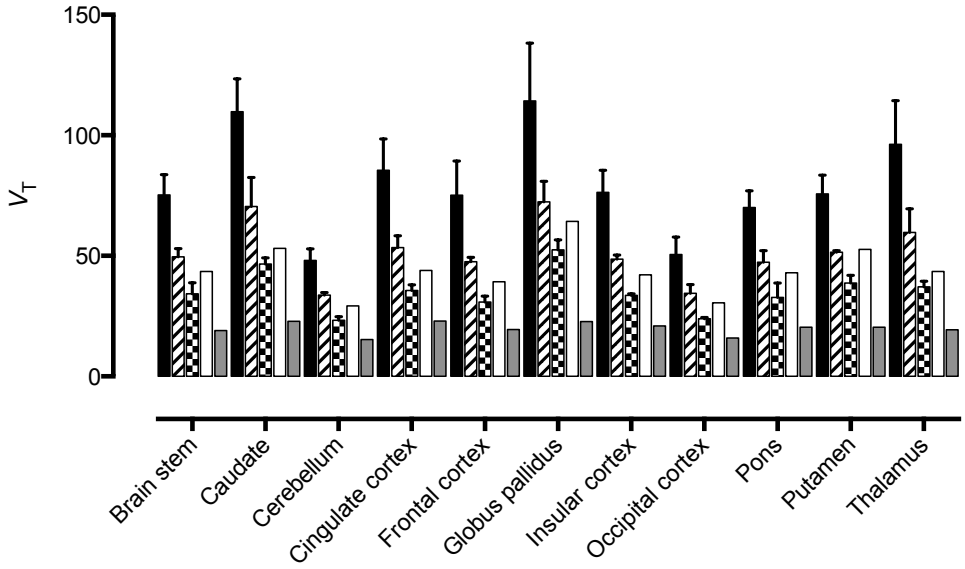

Figure 6. Dose dependent occupancy by BU224 in whole brain, occupancy calculated using the occupancy plot {Cunningham, 2010 #900} ED_{50}=0.022mg/kg). V_T data generated using the MA1 model; monkey 1 ● , monkey 2 ○ .